Journal of Food and Drug Analysis

Volume 31 | Issue 3 Article 9

# Identification for metabolism profiles and pharmacokinetic studies of tradition Chinese prescription Ji-Ming-San and its major metabolites in rats by UHPLC-Q-TOF-MS/MS and UHPLC-MS/MS

ORIGINAL ARTICLE

# Identification for metabolism profiles and pharmacokinetic studies of tradition Chinese prescription Ji-Ming-San and its major metabolites in rats by UHPLC-Q-TOF-MS/MS and UHPLC-MS/MS

Cheng-Yang Hsieh [a,b], Ching-Chiung Wang [a,c,d,e], Lemmuel L. Tayo [f], Po-Wei Tsai [g], Chia-Jung Lee [a,c,d,*]

[a] Program in Clinical Drug Development of Herbal Medicine, College of Pharmacy, Taipei Medical University, Taipei, 110, Taiwan
[b] Laboratory of Oncology, Pharmacy Practice and Sciences, Graduate School of Pharmaceutical Sciences, Tohoku University, Sendai, Japan
[c] Graduate Institute of Pharmacognosy, College of Pharmacy, Taipei Medical University, Taipei, 110, Taiwan
[d] Traditional Herbal Medicine Research Center, Taipei Medical University Hospital, Taipei, 110, Taiwan
[e] School of Pharmacy, College of Pharmacy, Taipei Medical University, Taipei, 110, Taiwan
[f] School of Chemical, Biological, Materials Engineering and Sciences, Mapúa University, Intramuros, Manila, 1002, Metro Manila, Philippines
[g] Department of Medical Science Industries, College of Health Sciences, Chang Jung Christian University, Tainan, 711, Taiwan

**Abstract**

**Ji-Ming-Shan (JMS) is a traditional prescription use for patients with rheumatism, tendons swelling, athlete's foot, diuresis and even gout. This study developed a rapid and sensitive method for the analysis of JMS chemical components in the Traditional Chinese medicine (TCM) prescription and in the serum samples of rats which were administered with the herbal extract. Two mass spectrometric approaches were used namely Ultra-performance liquid chromatography-quadrupole time-of-flight-mass spectrometry (UPLC-Q-TOF-MS) method for the major metabolites of the JMS extract while Ultra-performance liquid chromatography-tandem mass spectrometry (UPLC-MS/MS) was employed for the detection of the JMS metabolites in the sera of rats. It was revealed that the major components in the JMS extract were identified to be narirutin and hesperidin. It was confirmed that 17 compounds were determined in JMS prescription extract and 16 metabolites resulting from the biotransformation of narirutin and hesperidin were identified in the serum samples. *In silico* analyses also revealed that the metabolite hersperidin-7-glucoside exhibited the best binding ability with respect to the Cyclooxygenase-2 (COX-2) enzyme target. This study showcased the possible biochemical mechanism involved in the therapeutic efficiency of JMS components and their biotransformation products.**

*Keywords:* Hesperidin, Ji-Ming-Shan, Narirutin, UPLC-MS/MS, UPLC-Q-TOF-MS

## 1. Introduction

Traditional Chinese medicine (TCM) has created a landscape for the healthcare of many Asian people from different countries for a span of thousands of years [1]. TCM prescriptions have vast applications for many diseases but remains poorly understood in the scientific community because of insufficient evidence [2]. Several herbal components are typical in a TCM prescription and the need to elucidate their therapeutic mechanism in solitude or in combination with other components remain challenging [3]. Currently, the authenticity of the herbal medicine including their major components are documented in a database called Traditional Chinese Medicine Integrated Database or TCMID [4].

One popular TCM prescription is Ji-Ming-Shan (JMS) which has been extensively used for patients

Received 7 April 2023; revised 11 July 2023; accepted 30 July 2023.
Available online 31 August 2023

* Corresponding author at: Program in Clinical Drug Development of Herbal Medicine, College of Pharmacy, Taipei Medical University, Teaching & research building, 250 Wu-Hsing Street, Taipei, 110, Taiwan. Fax: +886 2 27361661 ext. 6185.
E-mail addresses: d339108001@tmu.edu.tw (C.-Y. Hsieh), crystal@tmu.edu.tw (C.-C. Wang), lltayo@mapua.edu.ph (L.L. Tayo), powei@mail.cjcu.edu.tw (P.-W. Tsai), cjlee@tmu.edu.tw (C.-J. Lee).

https://doi.org/10.38212/2224-6614.3473

with rheumatism, tendon swelling, foot pain, athlete's foot, diuresis, and gout [5−8]. JMS is composed of seven herbs which are: *Areca cathechu* Burm.f., *Citrus reticulata* Blanco, *Chaenomeles speciosa* (Sweet) Nakai, *Euodia ruticarpa* (A. Juss.) Benth., *Perilla frutescens* (L.) Britton, *Zingiber officinale* Roscoe, *Platycodon grandiflorus* (Jacq.) A.DC. Generally, this herbal prescription has been widely used for the treatment of inflammatory responses of the body [8].

Acute or chronic inflammation in the human body is brought about by a complex cascade of molecular and cellular events following an exposure from a noxious stimulus. Consequently, local tissue or systemic response can occur because of the many cascades of biochemical inflammatory reactions [9,10]. Inflammation is now identified as the key player for the development of diseases such as diabetes, cancer, cardiovascular diseases, autoimmunity, and even arthritis [11]. In the case of rheumatism, pre-clinical studies indicate that pro-inflammatory chemical factors produced by the chondrocytes, synovium, and other surrounding tissues play an important role in the inflammation leading to the disease [12]. Prostaglandins formed from arachidonic acid via the enzyme cyclooxygenase 2 (COX-2) plays a key role in their synthesis [13,14].

Another important study known as pharmacochemistry is an emerging field that uses a variety of modern instruments and tools for the separation and identification of potential functional components in serum [15,16]. Two important mass spectrometric tools are relevant for the rapid detection of TCM components. Ultra-high performance liquid chromatography-quadrupole time-of-flight-mass spectrometry (UPLC-Q-TOF-MS) mass spectrometry offers high accurate relative molecular mass detection while the triple quadrupole mass spectrometry (UPLC-MS/MS) demonstrate high sensitivity and high accuracy for the acquisition of molecular masses of the metabolites [16,17]. The instrumental designs limit their application where UPLC-Q-TOF-MS finds suitability for the measurement of relative molecular masses and convenience of usage is demonstrated in UPLC-MS/MS for pharmaceutical analysis [18−20]. With this sophisticated instrumentation, our study aims to analyze serum samples of animal models which are orally administered with the TCM prescription JMS.

Currently, biochemical mechanisms involved in the therapeutic efficacies of JMS have not been established in the scientific literature. This study aims to develop a rapid and innovative mass spectrometry platform for studying JMS *in vivo*. UPLC-Q-TOF-MS mass spectrometry was use for the identification of components in the herbal prescription while the major metabolites of JMS in rat plasma was detected using a tandem mass spectrometric approach (UPLC-MS/MS). These serum metabolites were further verified by bioinformatics approaches such as molecular docking (MD) and Structure−Activity Relationship (SAR) to investigate the binding affinity and other interactions with respect to the protein target. This study can provide scientific insights on how JMS exert its therapeutic benefit to patients.

## 2. Materials and methods

### 2.1. Chemicals and reagents

Standards including hesperidin, narirutin were purchased from ChemFaces Co., Ltd. (Wuhan, China), and their purities were not lower than 99% according to HPLC analysis. Formic acid was purchased from (Merck, Germany). Chromatographic reagent Methanol (Merck, Germany) and acetonitrile (Merck, Germany) were used for LC/MS analysis. Deionized Water was purified by Milli-Q purification system (Millipore, MA, USA). All other chemical regents were of analytical grade.

### 2.2. Plant materials

The plant prescription is according to the Ministry of Health and Welfare each contained *A. cathechu* (8 g), *Citrus reticulata* (5 g), *C. speciosa* (5 g), *E. ruticarpa* (1.5 g), *P. frutescens* (1.5 g), *Z. officinale* (2.5 g), *P. grandiflorus* (2.5 g) all the herbals were obtained from Sun Ten Pharmaceutical Co., Ltd. and the quality were identified by Herbiotek CO., LTD.

### 2.3. Sample preparation and extraction

The prescription is in accordance with the Ministry of Health and Welfare. The Ji-Ming-Shan prescription contained seven herbs *A. cathechu, Citrus reticulata, C. speciosa, E. ruticarpa, P. frutescens, Z. officinale*, *Platycodon grandifloras*. All the medicinal herbs were crashed and immersed in 95% ethanol (obtained from echo chemical Co., Ltd.) through the ratio of 1:20 under reflux extraction at 80 °C for 2 h per twice run. The twice liquid extract was combined used rotary evaporator to dry the extract.

### 2.4. Instrumentation and conditions

#### 2.4.1. UPLC-Q-TOF-MS analysis condition

The chromatographic separation of the samples was performed on Waters SYNAPT G2-Q-TOF and ACQUITY UPLC system. The analysis inject volume

of serum sample was 5 μL for the separation on ACQUITY UPLC™ HSS T3 (100 mm × 2.1 mm id, 1.8 μm) (Waters Group, USA), the flow rates were 0.3 mL/min and the column temperature was set at 40 °C. The mobile phase was composed of acetonitrile (A) and hyper-pure water (B), and gradient elution was set as follows: 0–1 min, 5 to 5% (A), 1–30 min, 5–100% (A), 30–33 min, 100 to 100% (A), 33–33.1 min, 100 to 5% (A), 33.1–35 min, 5 to 5% (A), positive mode containing 0.1% v/v formic acid, negative mode containing 10 mM ammonium acetate in mobile phases. In continuum mode at arrange from 50 to 1800 Da. Maximum MS/MS number of the selected for a single MS scan are 5 ions. The collision energy is ramp mode. The lock-mass of leucine enkephalin in both ion mode $[M + H]^+ = 556.2771$, $[M-H]^- = 554.2615$ was used to monitor the accurate mass calibration during MS data acquisition.

*2.4.2. UPLC–MS/MS conditions*

The UPLC-MS/MS system consisting of ACQUITY UPLC and Waters Xevo Triple Quadrupole Mass Spectrometry (Waters Group, USA). The chromatographic separation was achieved on the ACQUITY UPLC™ HSS T3 (100 mm × 2.1 mm id, 1.8 μm) (Waters Group, USA), the flow rates were set as 0.3 mL/min and the column temperature was set at 40 °C. The mobile phase was composed of acetonitrile (A) and hyper-pure water (B), and gradient elution was set as follows: 0–0.1 min, 5 to 5% (A), 0.1–8 min, 5–100% (A), 8–9 min, 100 to 100% (A), 9–9.1 min, 100 to 5% (A), 9.1.10 min, 5 to 5% (A), containing 0.1% v/v formic acid in mobile phases. And each injection volume was 5.0 μL. The mass spectrometer was operated in negative mode for oxacillin (IS), hesperidin, narirutin. Quantification was obtained using multiple reaction monitoring (MRM) mode in negative MS/MS scan mode. The optimal MS parameters were as follows: Interface ESI, Desolvation Temperature of 450 °C; Disolvation gas glow: 900 L/Hr; Cone 150 L/h. MS/MS operating conditions were optimized by infusion of the standard solution with internal standard oxacillin (200 ng/mL) of each injection into the ESI source via a syringe pump. The optimal MRM parameters for these compounds are shown as Table 1.

*2.5. In vitro and in vivo study of JMS-95E components*

*2.5.1. Animals and housing*

Male Wistar Rats (200–250 g) were housed individually in polycarbonate cages in an environmentally controlled room at 25 ± 1 °C with a 12-h day and night cycle. The animal facilities and protocols were approved by the local ethics committee of Taipei Medical University with Approval No (LAC-2020-0208). All the animal experiments were followed with accordance of the Guide for the Care and Use of laboratory Animals of the National Institutes of Health with the Publication No. 85–23.

*Table 1. MRM detection in negative mode and parameters for the 2 compounds and IS.*

| Components | Precursorion | Cone | Collision energy (eV) | Production |
|---|---|---|---|---|
| Narirutin | 579.15 | 48 | 25 | 150.88; 270.97 |
| Hesperidin | 609.15 | 18 | 25 | 310.01; 324.99 |
| Oxacillin (IS) | 399.79 | 10 | 24 | 173.71; 216.55 |

*2.5.2. Animal biological sample collection and preparation*

After oral administration the JMS-95E they were transferred to and housed in rat holder (rodent restraint) for continuous 8 h studied. The plasma sample was added in MeOH in a ratio of 1:3 and vortexed for 5 min. The mixture was centrifuged at 4500 rpm at 4 °C for 10 min, and the supernatant was transferred to another Eppendorf and evaporated to dryness after redissolved in 200 μL of 100% MeOH filter for UPLC-Q-TOF-MS analysis. Throughout the study all individual animals were handled approximately 5 min every day.

*2.6. Constituent and metabolite analysis*

The UPLC-MS data for the JMS and continuous collected serum samples were normalized after imported to Progenesis QI software (Waters Corporation) to chromatographic peak detection and auto-alignment, after all the data was applied to identify functional compound with self-create database (343 data sheets) from seven herbals, HMDB, Chemspider and Metlin databases.

*2.7. Validation of the method using UPLC-MS/MS*

*2.7.1. Preparation of calibration curve standards and quality control samples*

The stock solutions of the mixed standards were prepared in methanol with the concentrations of hesperidin (500 μg/ml), narirutin (500 μg/ml), and oxacillin (IS) (500 μg/ml). All solutions were stored at 4 °C. The concentrations of each analyte in standard mixture solutions were as follows: 31.25 μg/ml for hesperidin, 31.25 μg/ml for narirutin, 200 μg/ml for oxacillin. After, the standard mixture was diluted to a series of concentration to 31.25, 15.62, 7.81, 3.90,

1.95, 0.97, 0.48 ng/mL as calibration curves. All the samples were stored at −80 °C until analysis.

*2.7.2. Biological sample preparation*

The rat plasma sample 200 μL were added with MeOH in a ratio of 1:3 and vortexed for 5 min. The mixture was centrifuged at 4500 rpm at 4 °C for 10 min, and the supernatant was transferred to another Eppendorf tube and evaporated to dryness, redissolved in 200 μL of 100% MeOH and filtered for UPLC-MS/MS analysis.

*2.7.3. Method validation*

This method was validated according to the current FDA Bioanalytical Method Validation Guidance [21]. The following parameters were determined: specificity, selectivity, precision, accuracy, linearity range, LLOQ, LOD, extraction recovery rate, matrix effect, and stability test.

*2.7.4. Specificity and selectivity*

Rat blank plasma samples and samples spiked with the IS were examined for endogenous or IS interference. Specificity and selectivity were investigated by comparing the chromatograms of six individual batches of the rat blank plasma samples, plasma samples were added with the 2 analytes and IS, and plasma samples 60 min after oral administration of JMS.

*2.7.5. Linearity parameters*

To measure the linearity ranges, a series mixed of the standard solutions (seven concentrations) were prepared in triplicate. Each calibration curve ($y = ax + b$) was calculated by plotting the peak area ratio of analyte (y) to IS against the plasma concentration (x) of the analytes with a weighted (1/x) least square linear regression. The limit of quantification (LOQ) was conformed on the standard concentration curve with an acceptable accuracy (relative error $\leq \pm$ 15%) and a precision (relative standard deviation $\leq \pm$ 15%) and ten times of the background noise for LLOQ (lower limit of quantification) was required to be within ±20%. The limit of detection (LOD) was confirmed by the peak height (relative error $\geq \pm$ 20%) and a precision (relative standard deviation $\geq \pm$ 20%) and three times of the background noise, respectively.

*2.7.6. Precision and accuracy*

The intra- and inter-day precisions were conducted by RE, RSD, and developed by examined three concentrations levels of standard samples. Three samples were measured for each concentration level on the same day and the three continues other days, respectively. The analytic precision was conducted as the RSD, and the accuracy was considered the RE of the measured average standard deviation from each value. The acceptable criterion for the RSD was required to be $\leq \pm$ 15%, and the RE was required to be $\leq \pm$ 15%.

*2.7.7. Matrix effect and recovery rate*

The matrix effects were examined by compared the peak areas of the plasma matrix added with working standard solutions with the pure standard solutions in solvent at the same concentrations. The extraction recovery of the sample was calculated by compared the peak areas of pre-extraction plasma added standard solutions sample with the standard solutions plasma extraction at three QC levels.

*2.8. Pharmacokinetics*

After oral administered of herbal prescription blood samples were collected from the jugular vein using dried heparinized tubes at 0, 0.083, 0.167, 0.25, 0.5, 0.75, 1, 1.5, 2.0, 2.5, 3.0, 3.5, 4.0, 5.0, 6.0, 7.0, 8.0 and 24.0 h. The blood samples were then immediately centrifuged at 4500 rpm for 10 min. After the plasma was frozen and stored at −80 °C until analysis. The sample preparation was as 2.5.2 described for UPLC-MS/MS analysis.

*2.9. Stability test*

The stabilities of the 2 analytes in rat plasma was evaluated by assaying three replicates of QC samples at low, middle, and high concentrations in different experimental conditions: samples post-preparation stored in auto-sampler condition for 12 h, and storage at −80 °C for 7 days. The freeze-thaw stability was determined after the experience of three freeze–thaw cycles (from −80 °C to room temperature). Samples were identified as stable if the accuracy bias was within $\leq \pm$ 15.0% of the nominal concentration.

*2.10. In silico analysis (for COX-2:5KIR)*

*2.10.1. Ligand preparation*

The three-dimensional structure (in sdf file) of 16 structures: HMDB0014473 (Indomethacin), HMDB0030747 (Hesperetin 7-glucoside), HMDB0003265 (Hesperidin), HMDB0030748 (Hesperetin 7-neohesperidoside), HMDB0029203 (Hesperetin-7-O-Glucuronide), HMDB0041743 (Hesperetin 3′-O-Glucuronide), HMDB0240523 (Hesperetin 5-Glucuronide),

HMDB0033740 (Narirutin), HMDB0029209 (Naringenin-7-O-Glucuronide), HMDB0041759 (Naringenin 4′-O-Glucuronide), HMDB0037581 (Naringenin 5-O-Rhamnoside), HMDB0240547 (Naringenin 7-Sulfate), HMDB0304071 (2-Hydroxyisoflavanone Naringenin), HMDB0029631 (Naringenin chalcone), HMDB0035426 ((S)-Naringenin 8-C-(2″-rhamnosyl-glucoside)), HMDB0302091 ((2S)-Naringenin 8-C-alpha-L-rhamnopyranosyl-(1->2)-beta-D-glucopyranoside) were obtained from HMDB (https://hmdb.ca/) for docking analysis.

#### 2.10.2. Protein preparation and validation

Proteins were obtained from Protein Data Bank (PDB, https://www.rcsb.org/) and processed in Biovia Discovery studio 2022 and Pymol tools 2.5. The binding site and X-Y-Z coordinates of COX-2 (5KIR) [22] protein were defined in Biovia Discovery Studio and listed in Table 2.

#### 2.10.3. Molecular docking analysis

A Window 10 computer system with NVIDIA GeForce RTX 3050, AMD Ryzen 5 4600H, and 16.00 GB RAM were used for performing docking analysis on Biovia Discovery studio 2022 for analysis the LibDock score, binding ability of ligand binding sphere and protein, two-dimensional interaction.

### 2.11. Statistical analysis

All data were expressed as the mean ± SD. The plasma concentration of the investigated compounds was calculated by the calibration curve. The pharmacokinetic parameters, including Cmax (the peak of highest drug plasma concentration), Tmax (time to Cmax), AUC 0-t (the plasma concentration curve area from 0 to latest time point), AUC 0−inf (the plasma concentration curve area from 0 to infinity), MRT 0−inf (average residence time from 0 to latest infinity), and t1/2 (the concentration elimination half-life) all the data were calculated by a non-compartment model using the PKsolver. Statistical analysis was analysis by (Software: Graph pad Prism version-9; Excel 2019).

*Table 2. Protein target for docking analysis.*

| Target | PDB code | Grid parameters of the Binding Site | | Reference |
|---|---|---|---|---|
| | | coordinates | size | |
| COX-2 | 5KIR | x = 22.43<br>y = 27.49<br>z = 40.53 | x = 11<br>y = 11<br>z = 11 | [22] |

## 3. Result and discussion

### 3.1. Identification of in vitro JMS-95E and in vivo serum samples constituents

#### 3.1.1. Identification of the major components in JMS-95E by UPLC-Q-TOF-MS

The TIC (total ion chromatogram) in both ion modes were obtained by UPLC-Q-TOF-MS with Masslynx 4.0 (Fig. 1A−B and Tables 3−4). The ions of the compound are analyzed by auto pick peaking in the form of adduct ions $[M+H]^+$, $[2M + H]^+$, $[M-H]^-$ and $[2M-H]^-$. After the analysis 17 compounds were determined in JMS through positive and negative mode. 8 compounds were from *Citrus reticulata*, 2 compounds were from *C. speciosa,* 3 compound was from *E. ruticarpa*, 2 compounds were from *P. grandifloras,* 2 compounds were from *P. frutescens*.

#### 3.1.2. Identification of functional compounds in JMS-95E by UPLC-Q-TOF-MS

Due to the different platforms used in the instrumental design, we chose UPLC-Q-TOF-MS for qualitative and UPLC-MS/MS for quantitative analyses. In the qualitative part, we have sorted out our in-house database system curated from several scientific journals [23−33], and compared with online databases. Serum samples were collected for metabolite identification analysis from the TIC (total ion chromatogram). The blank group and the drug-administered group were determined by UPLC-Q-TOF-MS, though Progenesis-QI of the mass and MS/MS fragment analysis. Finally, a total of 16 compounds were determined in positive and negative mode (Fig. 2A−B and Tables 5−6). Biotransformation pathways recorded Phase1 and Phase 2 products for narirutin including glucuronidation (orange arrow), sulfation (black arrow), oxidation (blue arrow) (Fig. 3). The hesperidin metabolism pathway also including oxidative and glucuronidated product (orange arrow) and a sole glucuronide (red arrow) (Fig. 4). UPLC-Q-TOF-MS with automated data analysis for the P-QI analysis of the major components in JMS-95E and metabolic profile of rat plasma after oral administration result show that a total of 16 metabolites were identified and their characteristic fragmentations were summarized in Tables 5−6 and Figs. 3 and 4. In the previous study, 2 major compounds have been identified in JMS prescription. A rapid and selective LC/MS/MS method was developed for their analysis in the plasma sample. One major component being Narirutin (P5) undergoes xenobiotic biotransformation such as oxidation, glucuronidation to naringenin,

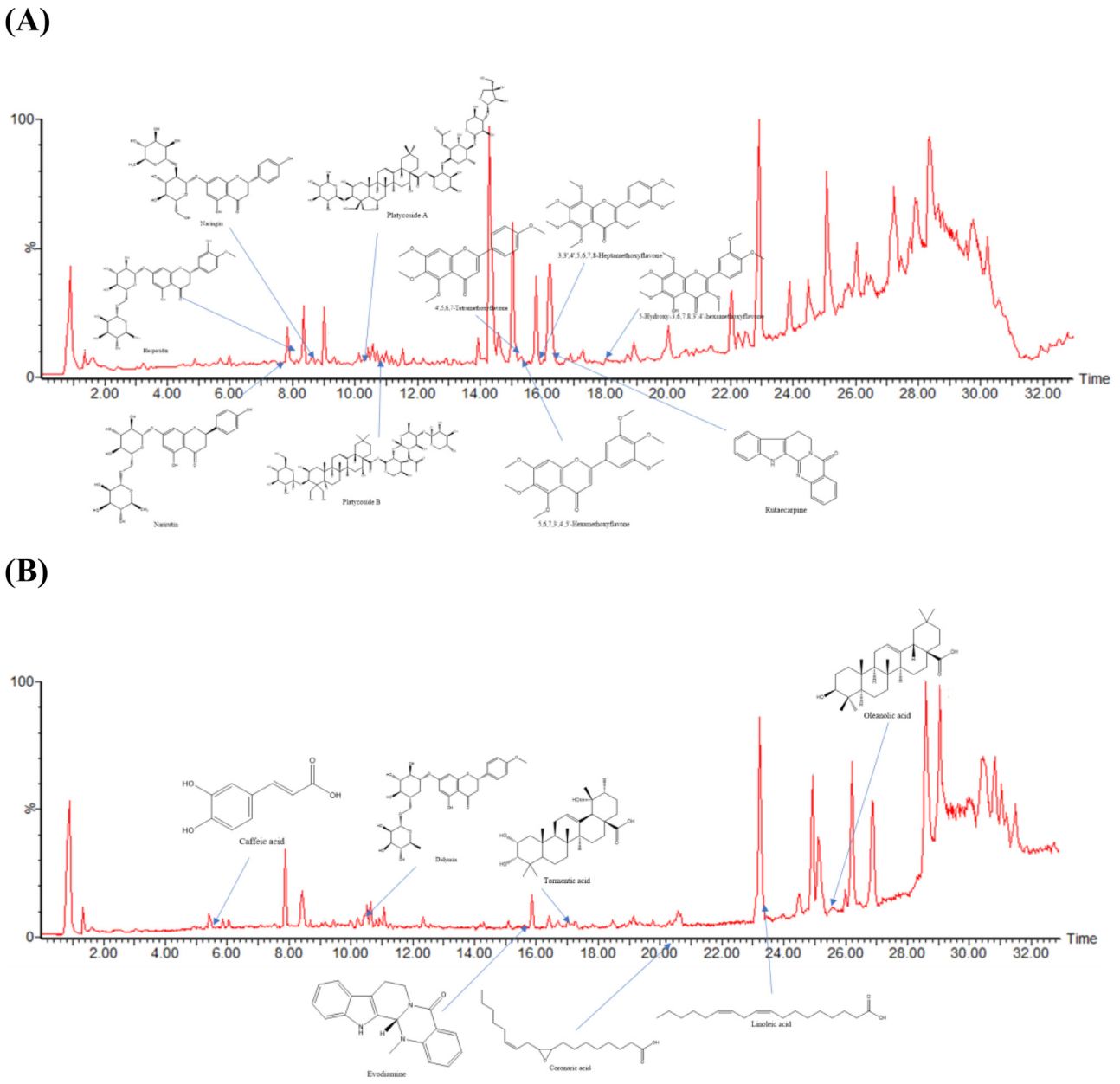


*Fig. 1. ESI chromatogram of identified components in JMS-95E. (A) The components JMS-95E using positive mode; (B) The components JMS-95E using negative mode.*

conjugation to glucuronides (PS1, PS2, PS10, NS2, NS3), sulfation (PS3) and oxidation to PS4. The second major metabolite in JMS, Hesperidin (P6) underwent oxidation and glucuronidated to hesperitin and Phase 2 metabolites are mainly from glucuronidation process (PS7, NS4, NS5, NS6) [34,35]. Flavonoids are primarily metabolized *in vivo* by phase II enzymes primarily found in the liver which includes glucosyltransferases (SbUGTs), glucuronosyltransferases (SbUGATs) and sulfotransferases (SULTs) which convert parent compounds to glucuronides and sulfated metabolites [36–38]. The bioavailability of flavonoid glycosides is quite low because of the high rate of biotransformation *in vivo*. Therefore, the bioavailability of flavonoid glycosides should include the xenobiotic biotransformation metabolites [39–41].

### 3.2. Validation of UPLC-MS/MS method

#### 3.2.1. Specificity

Typical chromatograms of blank, spiked plasma and plasma sample are shown in Fig. 5A–C. Results show that no interference was found between the

*Table 3. Identified Components of JMS-95E from positive ion mode.*

| Component | Classify | Identification | $t_R$ (Min) | Detected mass | Selected Ion | Formula | Fragment Ions (*m/z*) | Error (ppm) |
|---|---|---|---|---|---|---|---|---|
| P1 | Flavonoid | Narirutin | 7.80 | 581.1867 | M + H | $C_{27}H_{32}O_{14}$ | 273.0772, 271.0616, 263.0552, 147.0460 | −1.51 |
| P2 | Flavonoid | Hesperidin | 8.32 | 611.1966 | M + H | $C_{28}H_{34}O_{15}$ | 303.0864, 177.0544, 263.0551, 245.0446 | −2.45 |
| P3 | Flavonoid | Naringin | 8.62 | 581.1874 | M + H | $C_{27}H_{32}O_{14}$ | 273.0788, 457.1400 | −0.30 |
| P4 | Triterpenes | Platycodin A | 10.58 | 1267.5959 | M + H | $C_{59}H_{94}O_{29}$ | 455.3117, 129.0525, 587.3615, 97.0268 | −0.43 |
| P5 | Triterpenes | Platycoside B | 10.96 | 1135.5521 | M + H | $C_{54}H_{86}O_{25}$ | 485.285, 171.0666, 85.0298, 455.3149, | −1.84 |
| P6 | Flavonoid | 5,6,7,3′,4′, 5′-Hexamethoxyflavone | 15.04 | 403.1395 | M + H | $C_{21}H_{22}O_8$ | 403.1361, 388.1163, 370.1046 | −0.84 |
| P7 | Flavonoid | 4′,5,6, 7-Tetramethoxyflavone | 15.05 | 343.1180 | M + H | $C_{19}H_{18}O_6$ | 343.1174, 327.0830, 310.0870, 312.1031 | −2.07 |
| P8 | Flavonoid | 3,3′,4′,5,6,7, 8-Heptamethoxyflavone | 15.78 | 433.1500 | M + H | $C_{22}H_{24}O_9$ | 419.1347, 404.1106, 386.0977, 403.1015 | −0.93 |
| P9 | Alkaloid | Rutaecarpine | 16.24 | 288.1141 | M + H | $C_{18}H_{13}N_3O$ | 288.1123, 273.0886, 270.1031, 260.1171 | −0.47 |
| P10 | Flavonoid | 5-Hydroxy-3,6,7,8,3′, 4′-Hexamethoxyflavone | 18.02 | 419.1338 | M + H | $C_{21}H_{22}O_9$ | 419.1347, 404.1106, 386.0977, 403.1015 | −2.28 |

sample and plasma. Our method demonstrated two single sharp peaks at the retention time of narirutin, hesperidin and oxacillin (IS) which were 3.20, 3.35 and 5.01 min, respectively.

### 3.2.2. Linearity and sensitivity

In Table 7, linear equations are taken as follow: $y = 1060.7x + 583.99$, $R^2 = 0.9984$ for narirutin and $y = 1046.5x + 315.79$, $R^2 = 0.9990$ for hesperidin. The LLOQ of narirutin and hesperidin were 0.48 ng/mL while the LOD of narirutin and hesperidin were 0.125 ng/mL respectively. The linear regression both of compounds are summarized in Table 7. Within the investigated linear range, good linearity of data was obtained with correlation coefficients >0.9980. The results showed the UPLC-MS/MS method has a wide linear range and high sensitivity.

### 3.2.3. Precision and accuracy

As shown in Table 8 the precision and accuracy results for the intra-day precisions varied from 1.90 to 6.64% and the accuracy ranged from −5–97 to 8.75%. Inter-day precisions ranged from 0.55% to 5.45%. While the accuracy between −12.25 and 5.45%. The precision and accuracy were all in the acceptable range with reference to the Bioanalytical Method Validation Guidance.

### 3.2.4. Extraction recovery and matrix effects

The extraction recovery rate and matrix effects are shown in Table 9. The recoveries were between 55.34 and 66.96%. The matrix effects were between 70.07 and 91.17%, respectively. The recovery rate indicates the efficiency of the sample extraction process [21]. These two samples have less polar

*Table 4. Identified components of JMS-95E from negative ion mode.*

| Component | Classify | Identification | $t_R$ (Min) | Detected mass | Selected Ion | Formula | Fragment Ions (*m/z*) | Error (ppm) |
|---|---|---|---|---|---|---|---|---|
| N1 | Hydroxycinnamic acid | Caffeic Acid | 5.41 | 359.0762 | 2M-H | $C_9H_8O_4$ | 161.0236, 135.0438, 133.0282, 259.0805 | −2.88 |
| N2 | Flavonoid | Didymin | 10.22 | 593.1877 | M-H | $C_{28}H_{34}O_{14}$ | 280.0757, 593.1860, 309.0768, 367.0862 | 0.20 |
| N3 | Alkaloid | Evodiamine | 15.85 | 302.1292 | M-H | $C_{19}H_{17}N_3O$ | 169.0761, 302.1290, 142.0651, 116.0512 | −2.27 |
| N4 | Triterpenes | Tormentic Acid | 16.67 | 487.3412 | M-H | $C_{30}H_{48}O_5$ | 487.3415, 469.3347, 444.3242, 427.3245 | −3.48 |
| N5 | Triterpenes | Corosolic Acid | 20.26 | 471.3472 | M-H | $C_{30}H_{48}O_4$ | 471.3478, 453.3372, 458.3286, 454.3413 | −1.66 |
| N6 | Fatty acid | Linolenic Acid | 23.31 | 277.2167 | M-H | $C_{18}H_{30}O_2$ | 277.2167, 259.2104, 233.2333, 181.1259 | −2.17 |
| N7 | Triterpenes | Oleanic Acid | 25.16 | 455.3527 | M−H, | $C_{30}H_{48}O_3$ | 455.3540, 303.2360 | −0.75 |

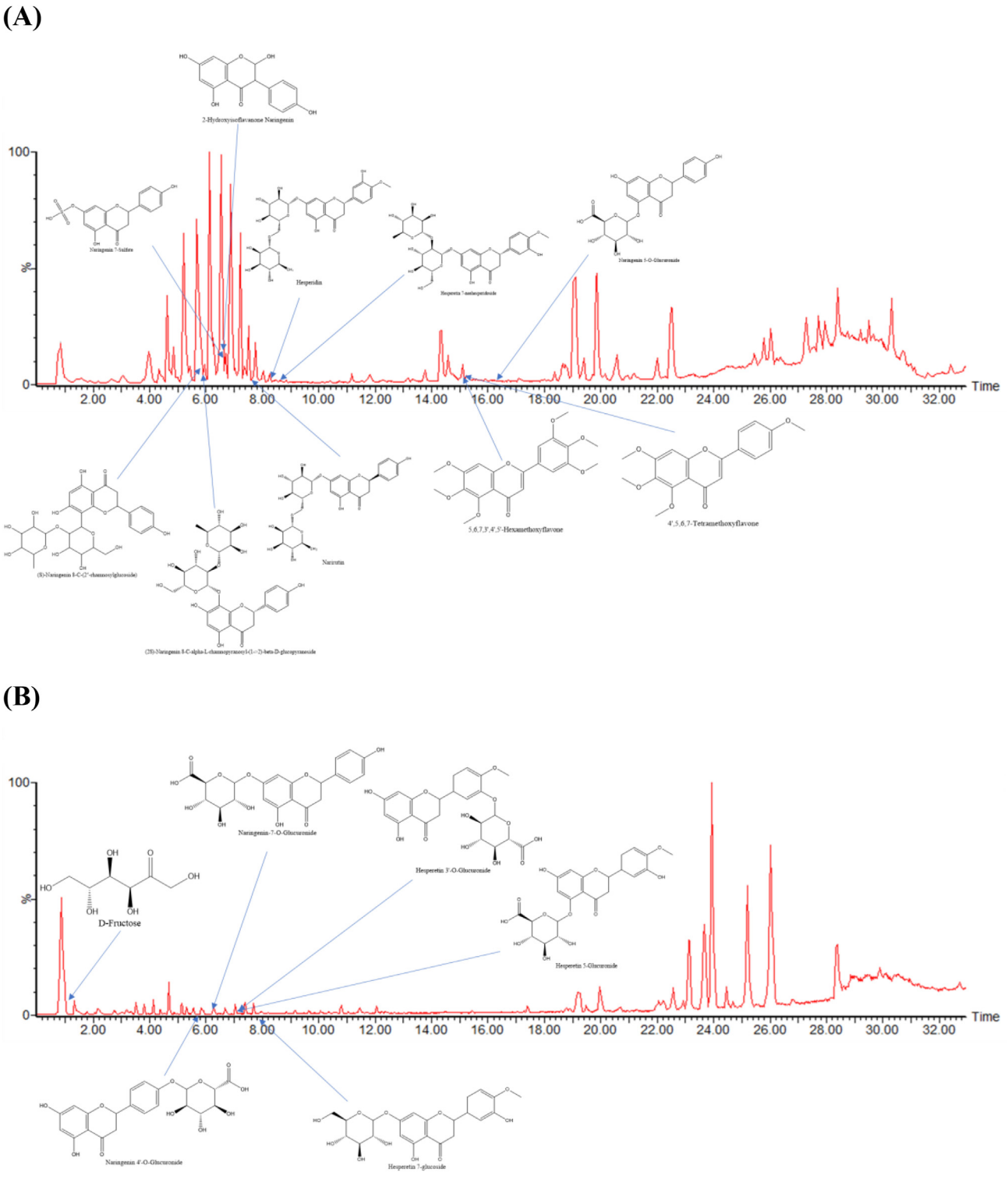


*Fig. 2. ESI chromatogram of the identified metabolites after orally administration of JMS-95E. (A) Functional components of JMS-95E identified using positive mode; (B) Functional components of JMS-95E identified using negative mode.*

properties, and the samples have a lower concentration in the blood. We tried various extraction methods such as liquid–liquid extraction and protein precipitation. We found that neither diethyl ether nor ethyl acetate was effective in improving recovery (data not shown), and acetonitrile at a reference ratio of 1:3 was the most suitable extraction method [42]. Spike recoveries ranged from

*Table 5. Identification of the metabolites from plasma positive ion mode after oral administration of JMS-95E.*

| Metabolite | Classify | Identification | $t_R$ (Min) | Detected mass | Selected Ion | Formula | Fragment Ions (*m/z*) | Error (ppm) |
|---|---|---|---|---|---|---|---|---|
| PS1 | Flavonoid | (S)-Naringenin 8-C-(2″-rhamnosylglucoside) | 5.95 | 581.1867 | M + H | $C_{27}H_{32}O_{14}$ | 273.0757, 285.0789, 315.0887, 85.0284 | −1.51 |
| PS2 | Flavonoid | (2S)-Naringenin 8-C-alpha-L-rhamnopyranosyl -(1->2)-beta-D-glucopyranoside | 5.95 | 581.1867 | M + H | $C_{27}H_{32}O_{14}$ | 273.0757, 339.0896, 71.0471,285.0789 | −1.51 |
| PS3 | Flavonoid | Naringenin 7-sulfate | 6.69 | 353.0331 | M + H | $C_{15}H_{12}O_8S$ | 273.0773, 271.0628 | −1.59 |
| PS4 | Flavonoid | 2-hydroxyisoflavanone naringenin | 6.99 | 289.0721 | M + H | $C_{15}H_{12}O_6$ | 153.0190, 179.0345, 254.0585, 147.0451 | 1.16 |
| PS5 | Flavonoid | Narirutin | 7.80 | 581.1867 | M + H | $C_{27}H_{32}O_{14}$ | 419.1339, 389.0878, 404.1104, 127.0358 | −1.51 |
| PS6 | Flavonoid | Hesperidin | 8.32 | 610.1894 | M + H | $C_{28}H_{34}O_{15}$ | 303.0864, 177.0544, 263.0551, 245.0446 | −2.45 |
| PS7 | Flavonoid | Hesperetin 7-neohesperidoside | 8.32 | 610.1894 | M + H | $C_{28}H_{34}O_{15}$ | 303.0864, 177.0544, 381.0991, 413.1215 | −2.45 |
| PS8 | Flavonoid | 5,6,7,3′,4′,5′-Hexamethoxyflavone | 15.04 | 403.1395 | M + H | $C_{21}H_{22}O_8$ | 403.1361, 388.1163, 370.1046 | −0.84 |
| PS9 | Flavonoid | 4′,5,6,7-Tetramethoxyflavone | 15.05 | 343.1180 | M + H | $C_{19}H_{18}O_6$ | 343.1174, 327.0830, 310.0870, 312.1031 | −2.07 |
| PS10 | Flavonoid | Naringenin 5-rhamnoside | 16.16 | 419.1342 | M + H | $C_{21}H_{22}O_9$ | 389.0872, 419.1349, 404.1113, 361.0928 | −1.32 |

53.93% to 74.74%, and although the ranges varied, all RSD values were below 15.00%. These data indicate that endogenous substances do not alter the analysis of rat plasma, and the UPLC-MS/MS method demonstrates its suitability for this analysis. In addition, matrix effects performed well in most samples, ranging from 88.40% to 97.30%, respectively. However, the lowest concentration of hesperidin (1 ng/mL) had lower matrix effects. Refer to other relevant literature Matrix effects may be caused by co-elution with analyte compounds [43,44].

#### 3.2.5. Stability test

The stability test in different experimental conditions is summarized in Table 10. Results showed all RSD% ranged from −0.63 to 7.78% and RE% were from −7.44 to 12.58%, which suggested that all analytical compounds were stable in rat plasma for 12 h in normal temperature after preparation, three freeze−thaw cycles and 1 month storage at −80 °C.

### 3.3. Pharmacokinetic study

At present, the plasma concentration of narirutin and hesperidin including its metabolites have not been documented in the scientific literature. We take advantage on the use UPLC-MS/MS for quantitative analysis since these metabolites occur in minute amounts in the serum sample. Our results showed that the two main substances are absorbed very quickly in the blood (Fig. 6 and Table 11). Narirutin and hesperidin were successfully identified in the plasma after oral administration JMS-

*Table 6. Identification of the metabolites from plasma negative ion mode after oral administration of JMS-95E.*

| Metabolite | Classify | Identification | $t_R$ (Min) | Detected mass | Selected Ion | Formula | Fragment Ions (*m/z*) | Error (ppm) |
|---|---|---|---|---|---|---|---|---|
| NS1 | Monosaccharides | D-Fructose | 0.87 | 341.1083 | M-H | $C_{12}H_{22}O_{11}$ | 59.0144, 113.0228, 145.0528, 143.0351 | −1.86 |
| NS2 | Flavonoid | Naringenin 4′-O -glucuronide | 5.79 | 447.0932 | M-H | $C_{21}H_{20}O_{11}$ | 271.0608, 165.0184, 113.0261, 252.0389 | −0.19 |
| NS3 | Flavonoid | Naringenin-7-O -glucuronide | 6.19 | 447.0927 | M-H | $C_{21}H_{20}O_{11}$ | 447.0940, 307.0427, 99.0093, 313.0681 | −1.30 |
| NS4 | Flavonoid | Hesperetin 5 -glucuronide | 7.10 | 477.1057 | M-H | $C_{22}H_{22}O_{12}$ | 113.0243, 477.1018, 195.0673 | 3.87 |
| NS5 | Flavonoid | Hesperetin 3′-O -glucuronide | 7.10 | 477.1057 | M-H | $C_{22}H_{22}O_{12}$ | 477.1018, 113.0243 | 3.87 |
| NS6 | Flavonoid | Hesperetin 7 -glucoside | 7.81 | 463.1260 | M-H | $C_{22}H_{24}O_{11}$ | 388.1157, 315.0990, 285.0780 | 3.05 |

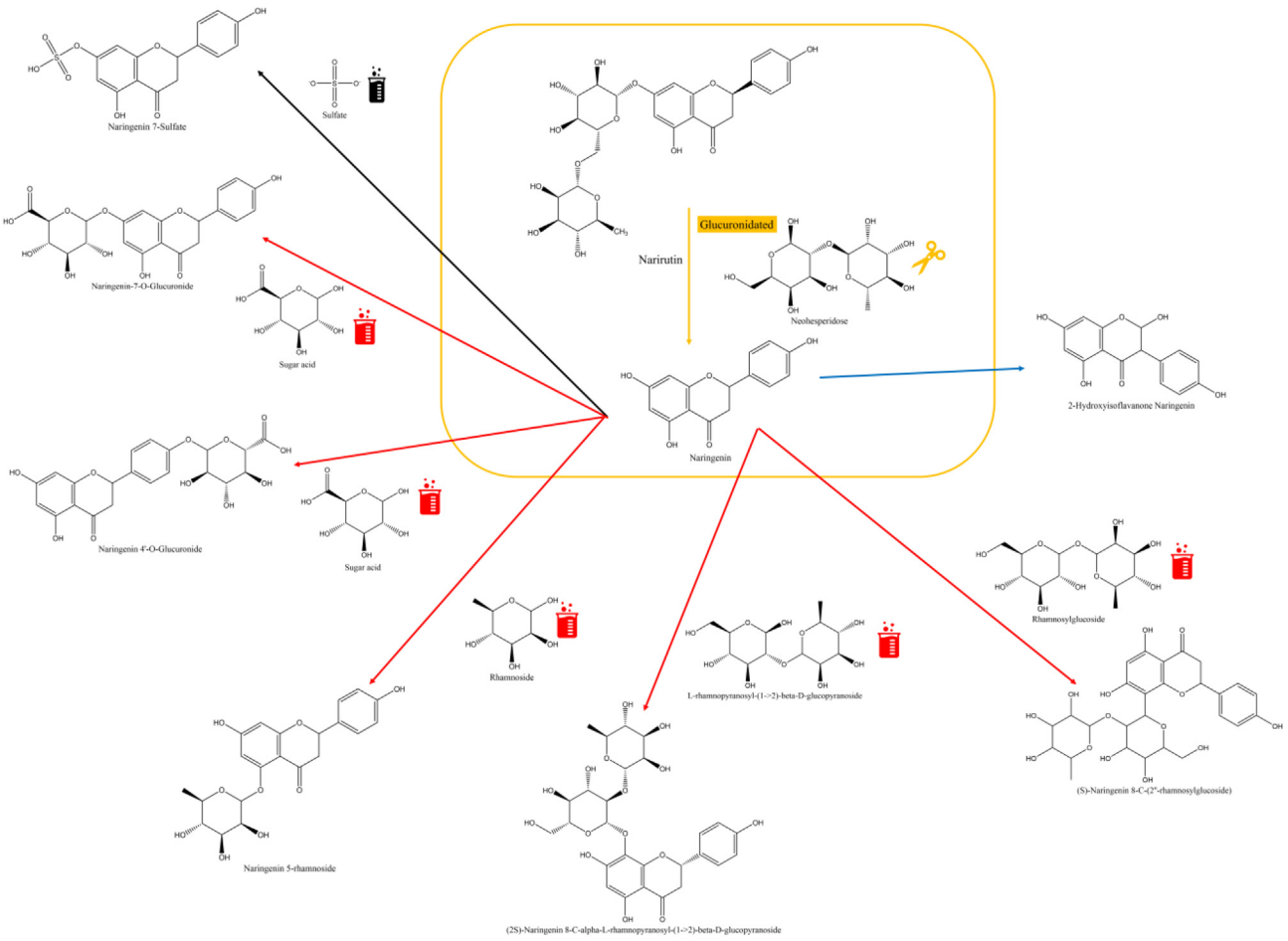


*Fig. 3. Proposed biotransformation pathway for Narirutin after oral administration of JMS-95E. Glucuronidation: Orange arrow, Sulfation: black arrow), Oxidation: Blue arrow, Beaker: Functional group added, Scissors: Functional group removed.*

95E. These results also confirmed that the two compounds are the pharmaceutically active components of JMS-95E. The effects of JMS-95E on plasma concentrations were evaluated by comparing the changes in PK parameters. The developed assay was sensitive enough for the pharmacokinetic analysis of the 2 components in rat plasma by oral administration of JMS-95E at a dose of 800 mg/kg. The time concentration curve of the 2 analytes in rat plasma had shown in Fig. 6A–B and the pharmacokinetic parameters were summarized in Table 11. By comparing the retention of the standards, we found that narirutin and hesperidin were absorbed in a rapid time in rats after oral administration of JMS extract (Fig. 6). Statistical analysis (non-compartmental model) showed that the major components of JMS were absorbed rapidly the Tmax (h) of narirutin and hesperidin is 1.01 ± 1.22, 1.1 ± 2.4 and Cmax (ng/ml) is 3.29 ± 1.63, 13.59 ± 7.7 (Table 11).

### 3.4. Molecular docking analysis

The docking analysis was performed to examine the binding affinity of JMS-95E metabolites with the target COX-2 proteins 5KIR with the non-steroidal anti-inflammatory drug indomethacin (see Fig. 7). In Table 12, Hesperetin 7-glucoside, Hesperidin Hesperetin 7-neohesperidoside, Hesperetin 3′-O-glucuronide, Hesperetin 5-glucuronide, Hesperetin, Narirutin, Naringenin-7-O-glucuronide, Naringenin 4′-O-glucuronide, Naringenin 5-rhamnoside, Naringenin 7-sulfate, 2-hydroxyisoflavanone naringenin demonstrated higher binding affinity with the target protein when compared to the control based from the LibDock score (Table 12). The compound hesperetin 7-glucoside (Fig. 9A–B) also exhibited higher binding affinity with the target protein when compared to hesperidin (Fig. 8A–B). Hydrogen bonding, Van der Waals interaction, Pi–Pi interactions were also observed between the interacting amino acids of

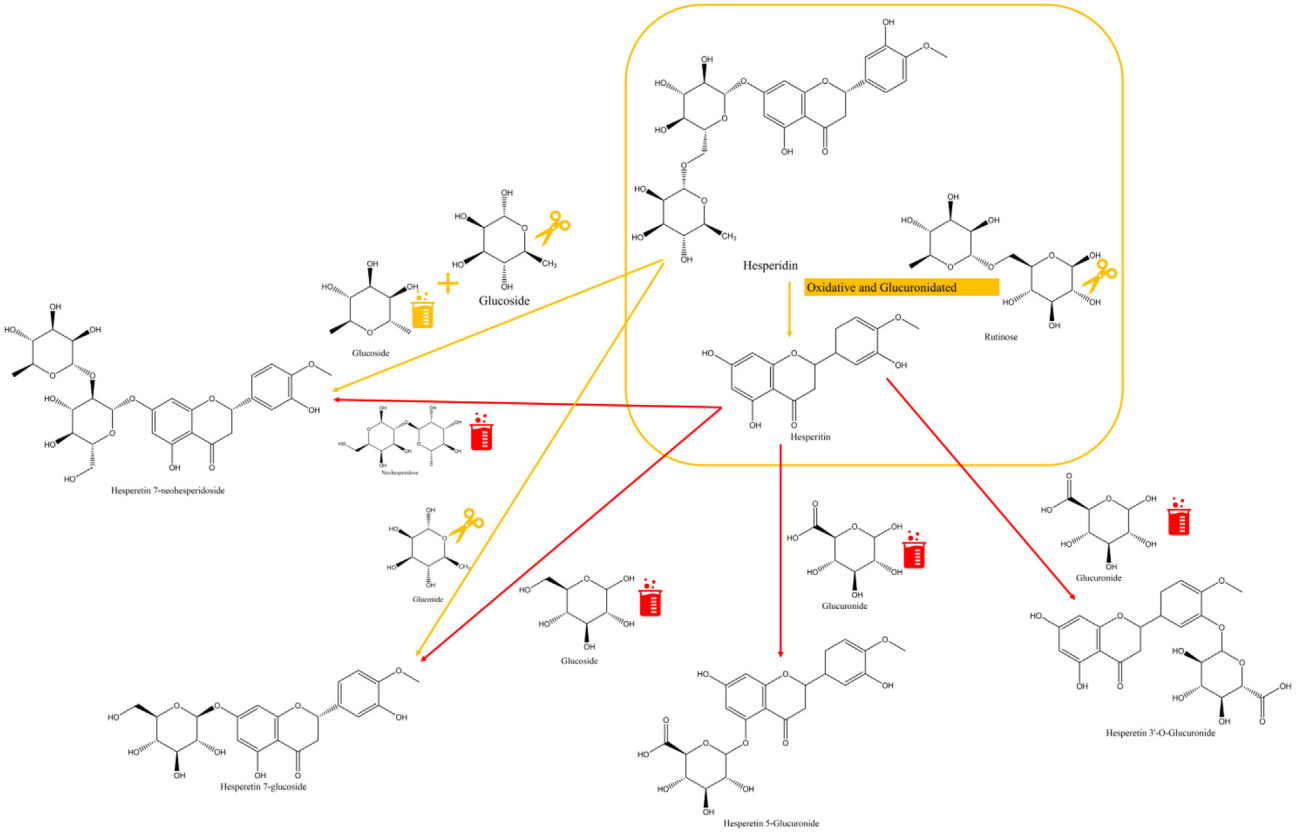


*Fig. 4. Proposed biotransformation pathway for Hesperidin after oral administration of JMS-95E. Oxidative and glucuronidated: orange arrow, Glucuronide: Red arrow, Beaker: Functional group added, Scissors: Functional group removed.*

COX-2 and JMS-95E metabolites (Table 13). After docking analysis, we found that the compound hesperetin 7-glucoside is more effective than hesperidin. Hesperetin 7-glucoside is a flavonoid monoglucoside which is produced by the enzyme α-rhamnosidase via the removal of the terminal rutinoside moiety [45,46]. Research has also shown that the bioavailability of hesperetin 7-glucoside via intestinal absorption is three-fold higher than hesperidin because of its higher solubility and two-fold better in suppressing the inflammation and growth *Helicobacter pylori* in the intestine and improve the health condition of DSS-induced colitis in mice with inflammatory bowel diseases [45–47].

All the metabolites demonstrated better binding affinity than the control COX-2 inhibitor drug indomethacin [48,49]. Through the ligand and COX-2 protein interaction hydrogen bonding the main active site is ARG44 of indomethacin (Fig. 7) and narirutin (Fig. 10). PI-Sulfur of CYS36 through indomethacin and hesperetin 7-glucoside. As the major compound Hesperidin had Van der Waals interaction and carbon hydrogen bond of the active sites involving CYS47, GLY135 of COX-2.

We further analyze the molecular docking analyses using structure–activity relationship (SAR) study. The chemical structure of flavonoids encounters cleavage of glycosidic residues *in vivo*, which leads to the increase in its bioavailability [50,51]. Similarly, Hesperidin and Narirutin aglycone structures Hesperetin and Naringenin exhibited lower Libdock scores than the glycone structure which means the cleavage of glycosidic bonds is primarily responsible for the enhanced bioavailability of the metabolites. The metabolite 2-hydroxyisoflavanone Naringenin has an isoflavone structure and studies has shown that this exert anti-inflammatory activity by reducing the production of chemical mediators (e.g.NF-κB, TNF-α, IL-1β, IL-6, iNOS, NO, COX-2 and PGE2) which are involved in the inflammatory process. In comparison with their flavone isomer counterparts at (C3), the latter has lower anti-inflammatory properties [52–55].

On the other hand, flavanone has a chemical structure which differ from the bond between C-2 and C-3 form of flavones, which are the typical structural forms found in many fruits where various

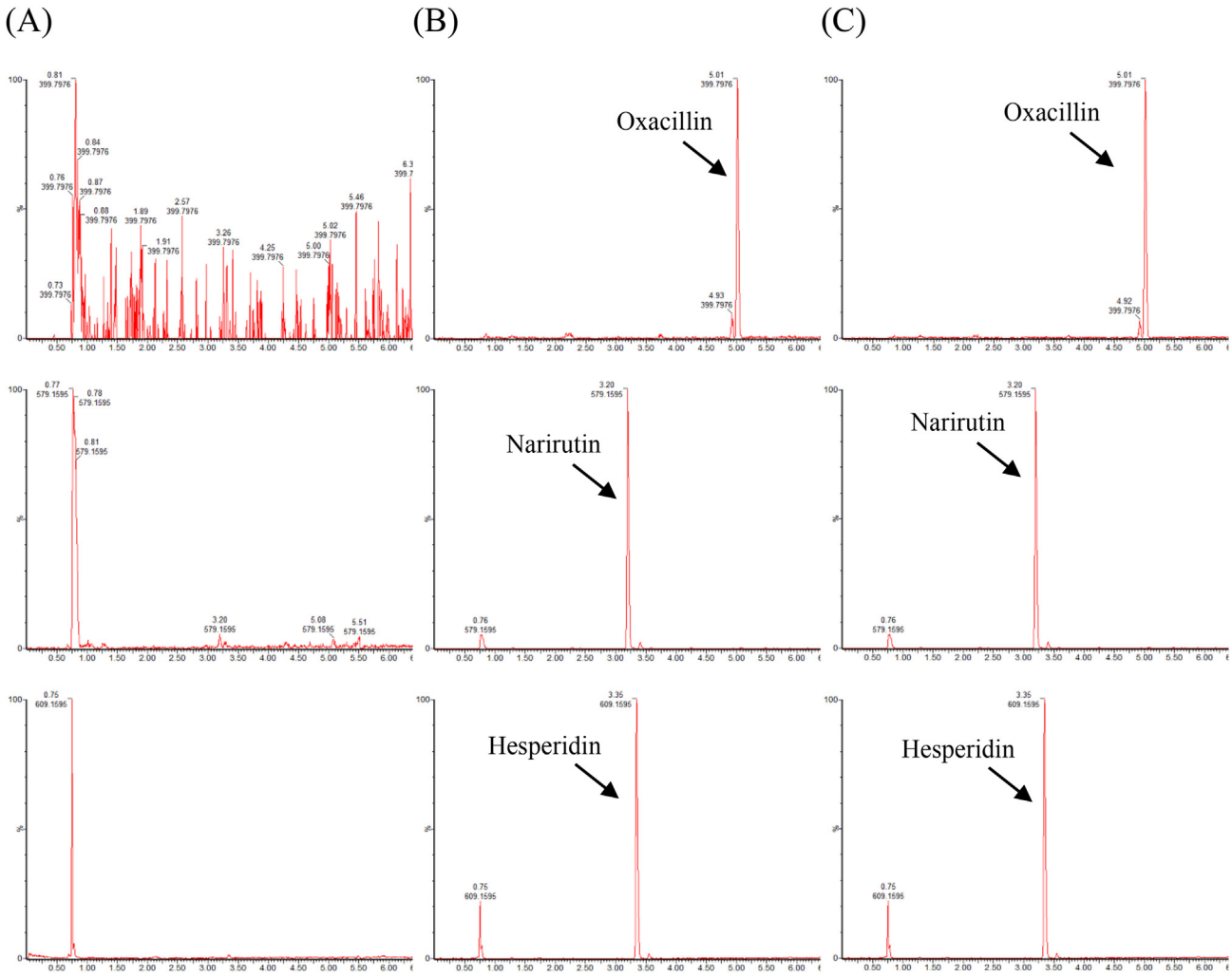


*Fig. 5. Representative multiple reaction monitoring (MRM) chromatograms of narirutin, hesperidin in vivo. (A) blank plasma, (B) blank plasma spiked with the 2 analytes, (C) 0.5 h after a oral administration of JMS-95E (800 mg/kg) to rats.*

*Table 7. Linear parameters of the compounds in rat plasma.*

| Components | Calibration curves | Correlation coefficients | Range (ng/mL) | LLOQ (ng/mL) | LOD (ng/mL) |
|---|---|---|---|---|---|
| Hesperetin | y = 1046.5x + 315.79 | $R^2$ = 0.9990 | 0.48–31.25 | 0.48 | 0.125 |
| Narirutin | y = 1060.7x + 583.99 | $R^2$ = 0.9984 | 0.48–31.25 | 0.48 | 0.125 |

*Table 8. Intra- and inter-day precisions and accuracies of JMS in rat plasma.*

| Analytes | Nominal conc (ng/mL) | Intra-day | | | Inter-day | | |
|---|---|---|---|---|---|---|---|
| | | Observed | Precision (RSD, %) | Accuracy (RE, %) | Observed | Precision (RSD, %) | Accuracy (RE, %) |
| Narirutin | 0.48 | 0.47 ± 0.02 | 3.81 | −3.49 | 0.45 ± 0.03 | 6.64 | 6.91 |
| | 15.62 | 16.36 ± 0.56 | 3.39 | 4.71 | 16.38 ± 0.45 | 2.73 | 4.86 |
| | 31.25 | 29.55 ± 0.40 | 1.36 | −5.44 | 29.38 ± 0.56 | 1.90 | −5.97 |
| Hesperidin | 0.48 | 0.43 ± 0.02 | 5.45 | −12.25 | 0.53 ± 0.03 | 5.45 | 8.75 |
| | 15.62 | 15.39 ± 0.23 | 1.48 | −1.50 | 15.97 ± 0.45 | 2.80 | 2.23 |
| | 31.25 | 29.26 ± 0.16 | 0.55 | −6.37 | 29.40 ± 0.41 | 1.39 | −5.91 |

*Table 9. Recovery and matrix effects of the 2 analytes in rat plasma.*

| Analytes | Nominal conc (ng/mL) | Recovery rate | | Matrix effect | |
|---|---|---|---|---|---|
| | | Mean ± SD % | RSD % | Mean ± SD % | RSD % |
| Narirutin | 1 | 60.52 ± 3.58 | 5.92 | 89.54 ± 0.78 | 0.87 |
| | 5 | 69.15 ± 0.36 | 0.52 | 88.40 ± 10.35 | 11.71 |
| | 25 | 53.93 ± 3.64 | 6.75 | 88.88 ± 1.10 | 1.24 |
| Hesperidin | 1 | 74.74 ± 2.68 | 3.58 | 70.07 ± 8.08 | 11.53 |
| | 5 | 72.91 ± 1.20 | 1.65 | 97.3 ± 3.16 | 3.25 |
| | 25 | 55.34 ± 0.75 | 1.35 | 91.17 ± 1.43 | 1.57 |

*Table 10. Stability of the 2 analytes in rat plasma after oral administration of JMS-95E.*

| Analytes | Nominal conc (ng/mL) | Observed | Normal temperature | | −80 FT | | | −80 | |
|---|---|---|---|---|---|---|---|---|---|
| | | | Precision (RSD, %) | Accuracy (RE, %) | Observed | Precision (RSD, %) | Accuracy (RE, %) | Observed | Precision (RSD, %) | Accuracy (RE, %) |
| Narirutin | 0.48 | 0.5 ± 0.01 | 2.45 | −7.44 | 0.5 ± 0.01 | 4.47 | −3.82 | 0.5 ± 0.01 | 3.45 | −1.48 |
| | 15.62 | 17.94 ± 0.15 | 1.23 | 11.32 | 17.94 ± 0.15 | 3.44 | 12.58 | 17.94 ± 0.15 | 1.13 | 9.87 |
| | 31.25 | 31.04 ± 0.22 | 0.63 | −2.84 | 31.04 ± 0.22 | 0.69 | −3.1 | 31.04 ± 0.22 | 1.05 | −3.53 |
| Hesperidin | 0.48 | 0.46 ± 0.04 | 7.63 | −3.14 | 0.44 ± 0.02 | 5.14 | −7.42 | 0.47 ± 0.04 | 7.78 | −2.24 |
| | 15.62 | 16.95 ± 0.23 | 1.33 | 8.49 | 17.11 ± 0.38 | 2.22 | 9.47 | 17.10 ± 0.38 | 2.22 | 9.43 |
| | 31.25 | 30.00 ± 0.31 | 1.02 | −3.99 | 30.47 ± 0.29 | 0.94 | −2.49 | 30.01 ± 0.69 | 2.29 | −3.97 |

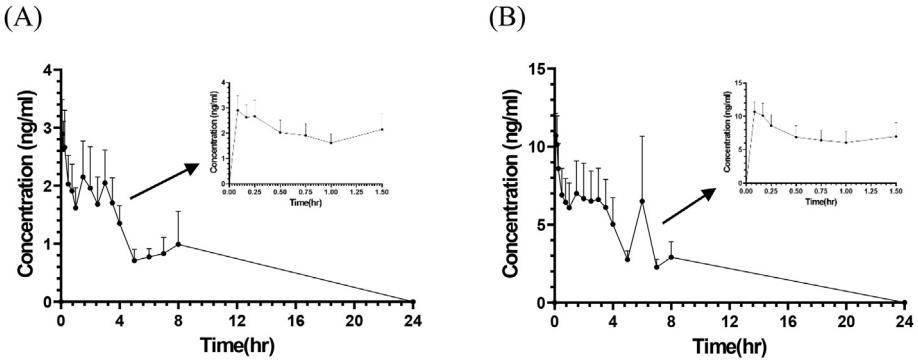


*Fig. 6. Profiles of the mean plasma concentration over time after oral administration of JMS-95E extract (800 mg/kg) to rats (Mean ± SD, n = 6) (A) Narirutin, (B) Hesperidin.*

*Table 11. Pharmacokinetic parameters of the 2 investigated compounds in rats after oral administration of JMS-95E.*

| | t1/2 (h) | Tmax (h) | Cmax (ng/mL) | AUC $_{0\text{-}t}$ (ng/mL*h) | AUC $_{0\text{-}inf}$ (ng/mL*h) | MRT $_{0\text{-}inf}$ (h) |
|---|---|---|---|---|---|---|
| Narirutin | 4.76 ± 1.76 | 1.01 ± 1.22 | 3.29 ± 1.63 | 11.01 ± 5.91 | 20.22 ± 11.93 | 8.22 ± 2.65 |
| Hesperidin | 4.39 ± 2.84 | 1.1 ± 2.40 | 13.59 ± 7.70 | 41.98 ± 25.77 | 58.61 ± 29.16 | 7.20 ± 3.16 |

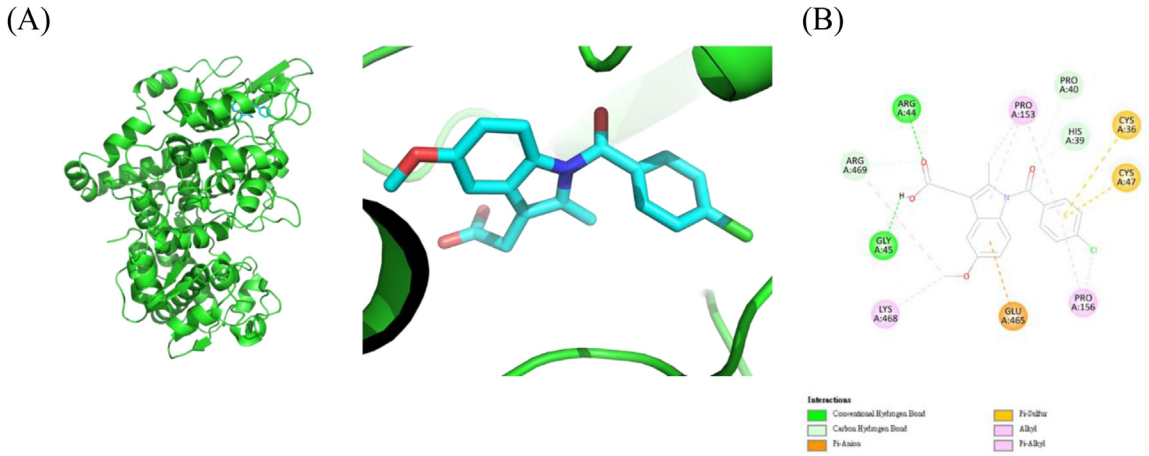


*Fig. 7. Binding interaction of 5KIR and Indomethacin (A) Ligand binding sphere and protein, (B) Two-dimensional display of the interaction.*

*Table 12. JMS Compounds with LibDock Scores for COX-2 (5KIR).*

| Selected Compounds | LibDock score |
|---|---|
| Indomethacin | 118.39 |
| Hesperetin 7-glucoside | 172.02 |
| Hesperidin | 169.42 |
| Hesperetin 7-neohesperidoside | 163.66 |
| Hesperetin 3′-O-glucuronide | 153.08 |
| Hesperetin 5-glucuronide | 143.23 |
| Hesperetin | 131.13 |
| Narirutin | 188.96 |
| Naringenin-7-O-glucuronide | 160.68 |
| Naringenin 4′-O-glucuronide | 152.55 |
| Naringenin 5-rhamnoside | 150.55 |
| Naringenin 7-sulfate | 123.39 |
| 2-hydroxyisoflavanone naringenin | 121.84 |
| Naringenin | 114.49 |
| (S)-Naringenin 8-C-(2″-rhamnosylglucoside) | – |
| (2S)-Naringenin 8-C-alpha-L-rhamnopyranosyl-(1->2)-beta-D-glucopyranoside | – |

* -: No LibDock score.

studies has shown their anti-inflammatory properties specially in citrus fruits [56–61]. The B-ring (3′ and 4′) containing hydroxyl groups in these flavanones can significantly suppress COX-2 transcription [62]. Another research demonstrated that flavonoids with the C-ring (C2–C3) with double bond and C4 with ketone group also fall under the class of flavanones. The Flavanones B-ring (3′ and 4’) with hydroxyl group or A-ring with 7-hydroxyl group has significantly more anti-inflammatory effect on COX-2 activity [62,63]. Same as the Libdock scores result of Hesperetin 7-glucoside, Hesperidin, Hesperetin 7-neohesperidoside, Narirutin and Naringenin-7-O-glucuronide have higher binding ability which translates to their anti-inflammatory properties. The A-ring with 6-hydroxyl group and substitution at C8 can influence inhibition of COX-2, owing to the torsional angle and coplanarity dilapidated [51,64]. It was also shown that (S)-Naringenin 8-C-(2″-rhamnosylglucoside) with 6-hydroxyl group of A-ring and substitution at C8 and (2S)-Naringenin 8-C-alpha-L-rhamnopyranosyl-(1->2)-beta-D-glucopyranoside had substitution at C8 and consequently led to poor inhibition with respect to COX-2.

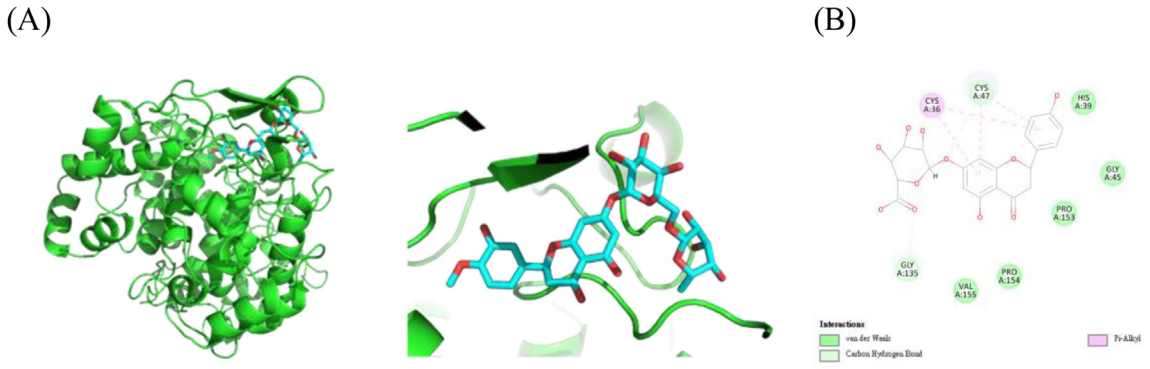


*Fig. 8. Binding interaction of 5KIR and Hesperidin (A) Ligand binding sphere and protein, (B) Two-dimensional display of the interaction.*

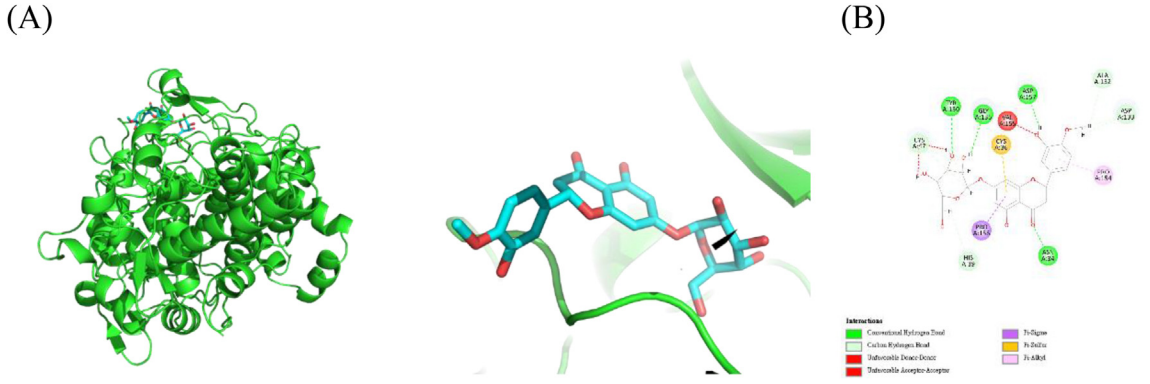


*Fig. 9. Binding interaction of 5KIR and Hesperetin 7-glucoside (A) Ligand binding sphere and protein, (B) Two-dimensional display of the interaction.*

*Table 13. Compounds interaction with COX-2 (5KIR) protein.*

| | Indomethacin | Hesperidin | Hesperetin 7-glucoside | Narirutin |
|---|---|---|---|---|
| Hydrogen Bonding | ARG44, GLY45 | N.A | ASN34, TYR130, GLY135, ASP157 | CYS36, ARG44, SER49, ALA151, VAL155, ASP157 |
| Carbon Hydrogen Bond | HIS39, PRO40, ARG469 | CYS47, GLY135 | HIS39, CYS47, ALA132, ASP133 | HIS39, MET48, GLY135, PRO156 |
| Van der Waals | N.A | HIS39, GLY45, PRO153, PRO154, VAL155 | N.A | N.A |
| Pi-Alkyl | PRO153, PRO156, LYS468 | N.A | PRO154 | PRO153, LEU152 |
| Pi -Anion | GLU465 | N.A | N.A | N.A |
| PI-Sulfur | CYS36, CYS47 | N.A | CYS36 | N.A |
| Pi-sigma | N.A | N.A | PRO156 | CYS47 |
| Unfavorable Donor −Donor | N.A | N.A | VAL155 | N.A |
| Unfavorable Acceptor −acceptor | N.A | N.A | VAL155 | N.A |

*N.A: Not applicable.

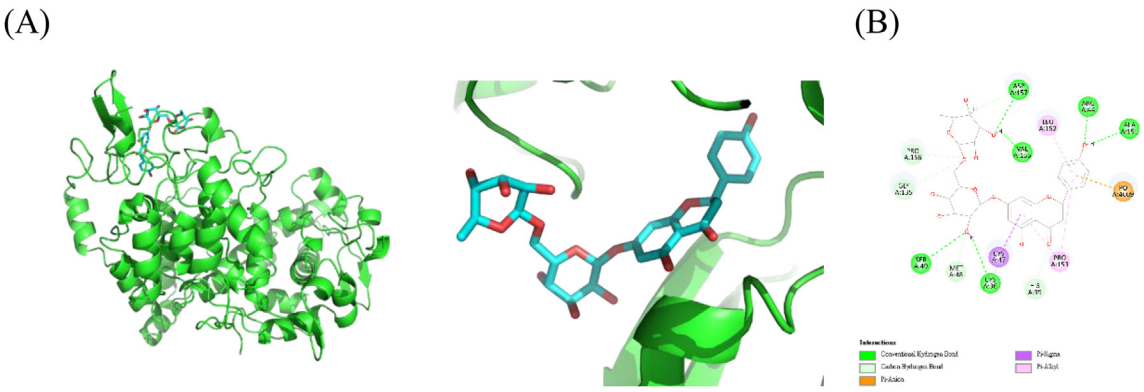


*Fig. 10. Binding interaction of 5KIR and Narirutin. (A) Ligand binding sphere and protein, (B) Two-dimensional display of the interaction.*

This study has led to identify secondary metabolites in the JMS extract and at the same time showcased biotransformation products of the major components of JMS in the serum of the rat models. The research platform employed can provide future insights on how therapeutic efficacy is achieved in other TCM prescription. This will hasten the scientific understanding on the biochemical mechanisms involved in therapeutic efficacies of other herbal prescriptions used in the practice of TCM. Furthermore, the instruments and methods in mass spectrometry including tools in bioinformatics altogether can hasten the scientific basis of TCM.

## 4. Conclusion

In this study, UPLC-Q-TOF-MS analysis showed the components in JMS-95E and metabolic profile of rat plasma of total of 17 components and 16 metabolites. The two main compounds are quickly absorbed in the blood. Narirutin oxidative and glucuronidated to naringenin and glucuronidated, sulfated, oxidative to other metabolites. Hesperidin oxidative and glucuronidated to hesperitin and glucuronidated to other metabolites. Docking result showed that hesperetin 7-glucoside are more effective than hesperidin and the compounds above are effective than celecoxib and indomethacin. JMS has been proven to exhibit anti-inflammatory properties. Therefore, we suggest that the narirutin, hesperidin, hesperetin 7-glucoside could be a potential functional compounds of JMS prescription.

## Conflict of interest

The authors declare that there are no conflicts of interest.

## Acknowledgments

Support for the present study came from the Taipei Medical University (TMU) of Ching-Chiung

Wang lab and Chia-Jung Lee lab's fund in support of the whole research. The authors thank Cheng-Yang Hsieh for writing original draft, investigation, data analysis and visualization. Ching-Chiung Wang for conceptualization. Lemmuel L. Tayo for reviewing the manuscript. And Po-Wei Tsai for writing review and editing.

## References

[1] Xu Q, Bauer R, Hendry BM, Fan T-P, Zhao Z, Duez P, et al. The quest for modernisation of traditional Chinese medicine. BMC Compl Alternative Med 2013;13:1–11.
[2] Zhang JH, Fan GW, Zhang H, Fan XH, Wang Y, Liu LM, et al. [Development and application of component-based Chinese medicine theory]. Zhongguo Zhongyao Zazhi 2017;42:4054–8. https://doi.org/10.19540/J.CNKI.CJCMM.2017.0161.
[3] Guoli W, Xuebao Z. A survey of the studies on compatible law of ingredients in Chinese herbal prescriptions. J Tradit Chin Med 2008;28:223–7. https://doi.org/10.1016/S0254-6272(08)60051-5.
[4] Huang L, Xie D, Yu Y, Liu H, Shi Y, Shi T, et al. Tcmid 2.0: a comprehensive resource for TCM. Nucleic Acids Res 2018;46:D1117–20. https://doi.org/10.1093/nar/gkx1028.
[5] Sun Y-X. Clinical application of jiming san. Chinese Journal of Basic Medicine in Traditional Chinese Medicine 2004;10:28–9.
[6] Ci H. Jiming San for the treatment of gout two two shells. Hubei Journal of Traditional Chinese Medicine 1994;3:52.
[7] Wang BOQING. ClinicaI observation on treatment of 3 6 cases of with modified JIMINGSAN gouty arthritisvol. 7; 2001.
[8] Hsieh C-Y, Wang C-C, Tayo LL, Deng S-X, Tsai P-W, Lee C-J. In vitro and in vivo anti-osteoarthritis effects of tradition Chinese prescription Ji-Ming-San. J Ethnopharmacol 2022:116084.
[9] Arulselvan P, Fard MT, Tan WS, Gothai S, Fakurazi S, Norhaizan ME, et al. Role of antioxidants and natural products in inflammation. Oxid Med Cell Longev 2016;2016:5276130. https://doi.org/10.1155/2016/5276130.
[10] Varela ML, Mogildea M, Moreno I, Lopes A. Acute inflammation and metabolism. Inflammation 2018;41:1115–27. https://doi.org/10.1007/s10753-018-0739-1.
[11] Sanchez-Lopez E, Coras R, Torres A, Lane NE, Guma M. Synovial inflammation in osteoarthritis progression. Nat Rev Rheumatol 2022;18:258–75. https://doi.org/10.1038/s41584-022-00749-9.
[12] Goldring MB, Otero M. Inflammation in osteoarthritis. Curr Opin Rheumatol 2011;23:471–8. https://doi.org/10.1097/BOR.0b013e328349c2b1.
[13] Ferrer MD, Busquets-Cortés C, Capó X, Tejada S, Tur JA, Pons A, et al. Cyclooxygenase-2 inhibitors as a therapeutic target in inflammatory diseases. Curr Med Chem 2019;26:3225–41. https://doi.org/10.2174/0929867325666180514112124.
[14] Simon LS. Role and regulation of cyclooxygenase-2 during inflammation. Am J Med 1999;106:37S–42S. https://doi.org/10.1016/s0002-9343(99)00115-1.
[15] Zhang C, Lian R, Mahmoodurrahman M, Lai S, Zhao Z, Yu Y. Serum pharmacochemistry for tracking bioactive components by UPLC-Q-TOF-MS/MS combined chromatographic fingerprint for quality assessment of Sanziguben Granule. J Chromatogr, B: Anal Technol Biomed Life Sci 2016;1029–1030:128–36. https://doi.org/10.1016/j.jchromb.2016.07.022.
[16] Xu L, Liu Y, Wu H, Wu H, Liu X, Zhou A. Rapid identification of chemical profile in Gandou decoction by UPLC-Q-TOF-MS(E) coupled with novel informatics UNIFI platform. J Pharm Anal 2020;10:35–48. https://doi.org/10.1016/j.jpha.2019.05.003.
[17] Zhao D, Yuan B, Carry E, Pasinetti GM, Ho L, Faith J, et al. Development and validation of an ultra-high performance liquid chromatography/triple quadrupole mass spectrometry method for analyzing microbial-derived grape polyphenol metabolites. J Chromatogr, B: Anal Technol Biomed Life Sci 2018;1099:34–45. https://doi.org/10.1016/j.jchromb.2018.09.014.
[18] Ens W, Standing KG. Hybrid quadrupole/time-of-flight mass spectrometers for analysis of biomolecules. Methods Enzymol 2005;402:49–78. https://doi.org/10.1016/S0076-6879(05)02002-1.
[19] Chernushevich I v, Loboda A v, Thomson BA. An introduction to quadrupole-time-of-flight mass spectrometry. J Mass Spectrom 2001;36:849–65. https://doi.org/10.1002/jms.207.
[20] Loos G, van Schepdael A, Cabooter D. Quantitative mass spectrometry methods for pharmaceutical analysis. Philos Trans A Math Phys Eng Sci 2016;374. https://doi.org/10.1098/rsta.2015.0366.
[21] Meesters R, Voswinkel S. Bioanalytical method development and validation: from the USFDA 2001 to the USFDA 2018 guidance for industry. J Appl Bioanal 2018;4:67–73.
[22] Orlando BJ, Malkowski MG. Crystal structure of rofecoxib bound to human cyclooxygenase-2. Acta Crystallogr F Struct Biol Commun 2016;72:772–6. https://doi.org/10.1107/S2053230X16014230.
[23] Li L, Luo Z, Liu Y, Wang H, Liu A, Yu G, et al. Screening and identification of the metabolites in rat plasma and urine after oral administration of Areca catechu L. Nut extract by ultra-high-pressure liquid chromatography coupled with linear ion trap-orbitrap tandem mass spectrometry. Molecules 2017;vol. 22. https://doi.org/10.3390/molecules22061026.
[24] Shi L, Wang R, Liu T, Wu J, Zhang H, Liu Z, et al. A rapid protocol to distinguish between Citri Exocarpium Rubrum and Citri Reticulatae Pericarpium based on the characteristic fingerprint and UHPLC-Q-TOF MS methods. Food Funct 2020;11:3719–29. https://doi.org/10.1039/d0fo00082e.
[25] Zhang J, Gao W, Liu Z, Zhang Z, Liu C. Systematic analysis of main constituents in rat biological samples after oral administration of the methanol extract of fructus aurantii by HPLC-ESI-MS/MS. Iran J Pharm Res (IJPR) 2014;13:493–503.
[26] Du H, Wu J, Li H, Zhong P-X, Xu Y-J, Li C-H, et al. Polyphenols and triterpenes from Chaenomeles fruits: chemical analysis and antioxidant activities assessment. Food Chem 2013;141:4260–8. https://doi.org/10.1016/j.foodchem.2013.06.109.
[27] Ling Y, Hu P, Zhang L, Jin H, Chen J, Tao Z, et al. Identification and structural characterization of acylgluconic acids, flavonol glycosides, limonoids and alkaloids from the fruits of evodia rutaecarpa by high performance liquid chromatography coupled to electrospray ionization and quadrupole time-of-fl. J Chromatogr Sci 2016;54:1593–604. https://doi.org/10.1093/chromsci/bmw109.
[28] Yuan J, Wei F, Luo X, Zhang M, Qiao R, Zhong M, et al. Multi-component comparative pharmacokinetics in rats after oral administration of fructus aurantii extract, naringin, neohesperidin, and naringin-neohesperidin. Front Pharmacol 2020;11:933. https://doi.org/10.3389/fphar.2020.00933.
[29] Wu J, Cui C, Zhang H, Liu D, Schreiber L, Qin W, et al. Identifying new compounds with potential pharmaceutical and physiological activity in Areca catechu and Areca triandra via a non-targeted metabolomic approach. Phytochem Anal 2021;32:970–81. https://doi.org/10.1002/pca.3039.
[30] Park SY, Jung MY. UHPLC-ESI-MS/MS for the quantification of eight major gingerols and shogaols in ginger products: effects of ionization polarity and mobile phase modifier on the sensitivity. J Food Sci 2016;81:C2457–65. https://doi.org/10.1111/1750-3841.13429.
[31] Wang C, Zhang N, Wang Z, Qi Z, Zhu H, Zheng B, et al. Nontargeted metabolomic analysis of four different parts of Platycodon grandiflorum grown in northeast China. Molecules 2017;22. https://doi.org/10.3390/molecules22081280.
[32] Gao X, Yang X-W, Marriott PJ. Evaluation of Coptidis Rhizoma-Euodiae Fructus couple and Zuojin products based on HPLC fingerprint chromatogram and simultaneous determination of main bioactive constituents. Pharm Biol 2013;51:1384–92. https://doi.org/10.3109/13880209.2013.793719.

[33] Lee YH, Kim B, Kim S, Kim M-S, Kim H, Hwang S-R, et al. Characterization of metabolite profiles from the leaves of green perilla (Perilla frutescens) by ultra high performance liquid chromatography coupled with electrospray ionization quadrupole time-of-flight mass spectrometry and screening for their antioxi. J Food Drug Anal 2017;25:776–88. https://doi.org/10.1016/j.jfda.2016.09.003.
[34] Shin K-C, Nam H-K, Oh D-K. Hydrolysis of flavanone glycosides by β-glucosidase from Pyrococcus furiosus and its application to the production of flavanone aglycones from citrus extracts. J Agric Food Chem 2013;61:11532–40. https://doi.org/10.1021/jf403332e.
[35] Nectoux AM, Abe C, Huang S-W, Ohno N, Tabata J, Miyata Y, et al. Absorption and metabolic behavior of hesperidin (Rutinosylated Hesperetin) after single oral administration to sprague-dawley rats. J Agric Food Chem 2019;67:9812–9.
[36] Pei T, Yan M, Li T, Li X, Yin Y, Cui M, et al. Characterization of UDP-glycosyltransferase family members reveals how major flavonoid glycoside accumulates in the roots of Scutellaria baicalensis. BMC Genom 2022;23:169. https://doi.org/10.1186/s12864-022-08391-1.
[37] Yao Y-F, Lin C-Z, Liu F-L, Zhang R-J, Zhang Q-Y, Huang T, et al. Identification and pharmacokinetic studies on complanatuside and its major metabolites in rats by UHPLC-Q-TOF-MS/MS and LC-MS/MS. Molecules 2018;24. https://doi.org/10.3390/molecules24010071.
[38] Chen Z, Zheng S, Li L, Jiang H. Metabolism of flavonoids in human: a comprehensive review. Curr Drug Metabol 2014;15:48–61. https://doi.org/10.2174/1389200215011402181250 20.
[39] Viskupičová J, Ondrejovič M, Šturdík E. Bioavailability and metabolism of flavonoids. J Food Nutr Res 2008;47.
[40] Hollman PCH. Absorption, bioavailability, and metabolism of flavonoids. Pharm Biol 2004;42:74–83.
[41] Thilakarathna SH, Rupasinghe HPV. Flavonoid bioavailability and attempts for bioavailability enhancement. Nutrients 2013;5:3367–87. https://doi.org/10.3390/nu5093367.
[42] Cortese M, Gigliobianco MR, Magnoni F, Censi R, Di Martino P Di. Compensate for or minimize matrix effects? Strategies for overcoming matrix effects in liquid chromatography-mass spectrometry technique: a tutorial review. Molecules 2020;25. https://doi.org/10.3390/molecules25133047.
[43] Zhou W, Yang S, Wang PG. Matrix effects and application of matrix effect factor. Bioanalysis 2017;9:1839–44.
[44] Gosetti F, Mazzucco E, Zampieri D, Gennaro MC. Signal suppression/enhancement in high-performance liquid chromatography tandem mass spectrometry. J Chromatogr A 2010;1217:3929–37.
[45] Lee Y-S, Huh J-Y, Nam S-H, Moon S-K, Lee S-B. Enzymatic bioconversion of citrus hesperidin by Aspergillus sojae naringinase: enhanced solubility of hesperetin-7-O-glucoside with in vitro inhibition of human intestinal maltase, HMG-CoA reductase, and growth of Helicobacter pylori. Food Chem 2012;135:2253–9.
[46] Wu F, Lei H, Chen G, Chen C, Song Y, Cao Z, et al. In Vitro and in vivo studies reveal that hesperetin-7-O-glucoside, a naturally occurring monoglucoside, exhibits strong anti-inflammatory capacity. J Agric Food Chem 2021;69:12753–62.
[47] Actis-Goretta L, Dew TP, Lévèques A, Pereira-Caro G, Rein M, Teml A, et al. Gastrointestinal absorption and metabolism of hesperetin-7-O-rutinoside and hesperetin-7-O-glucoside in healthy humans. Mol Nutr Food Res 2015;59:1651–62.
[48] Pitkeathly DA, Banerjee NR, Harris R, Sharp J. Indomethacin in in-patient treatment of rheumatoid arthritis. Ann Rheum Dis 1966;25:334–9. https://doi.org/10.1136/ard.25.4.334.
[49] Indomethacin. Bethesda (MD). 2012.
[50] Androutsopoulos VP, Tsatsakis AM. Benzo [a] pyrene sensitizes MCF7 breast cancer cells to induction of G1 arrest by the natural flavonoid eupatorin-5-methyl ether, via activation of cell signaling proteins and CYP1-mediated metabolism. Toxicol Lett 2014;230:304–13.
[51] Wang T-Y, Li Q, Bi K-S. Bioactive flavonoids in medicinal plants: structure, activity and biological fate. Asian J Pharm Sci 2018;13:12–23. https://doi.org/10.1016/j.ajps.2017.08.004.
[52] Wang X, Cao Y, Chen S, Lin J, Bian J, Huang D. Anti-inflammation activity of flavones and their structure–activity relationship. J Agric Food Chem 2021;69:7285–302.
[53] Yu J, Bi X, Yu B, Chen D. Isoflavones: anti-inflammatory benefit and possible caveats. Nutrients 2016;8:361.
[54] Panche AN, Diwan AD, Chandra SR. Flavonoids: an overview. J Nutr Sci 2016;5:e47.
[55] Kim HP, Son KH, Chang HW, Kang SS. Anti-inflammatory plant flavonoids and cellular action mechanisms. J Pharmacol Sci 2004;96:229–45.
[56] Kim HK, Cheon BS, Kim YH, Kim SY, Kim HP. Effects of naturally occurring flavonoids on nitric oxide production in the macrophage cell line RAW 264.7 and their structure–activity relationships. Biochem Pharmacol 1999;58:759–65.
[57] Teng J, Li Y, Yu W, Zhao Y, Hu X, Tao N, et al. Naringenin, a common flavanone, inhibits the formation of AGEs in bread and attenuates AGEs-induced oxidative stress and inflammation in RAW264. 7 cells. Food Chem 2018;269:35–42.
[58] Lee J-H. In-vitro evaluation for antioxidant and anti-inflammatory property of flavanone derivatives. Food Biosci 2015;11:1–7.
[59] Vafeiadou K, Vauzour D, Lee HY, Rodriguez-Mateos A, Williams RJ, Spencer JPE. The citrus flavanone naringenin inhibits inflammatory signalling in glial cells and protects against neuroinflammatory injury. Arch Biochem Biophys 2009;484:100–9.
[60] Chanet A, Milenkovic D, Manach C, Mazur A, Morand C. Citrus flavanones: what is their role in cardiovascular protection? J Agric Food Chem 2012;60:8809–22.
[61] Comalada M, Ballester I, Bailon E, Sierra S, Xaus J, Gálvez J, et al. Inhibition of pro-inflammatory markers in primary bone marrow-derived mouse macrophages by naturally occurring flavonoids: analysis of the structure–activity relationship. Biochem Pharmacol 2006;72:1010–21.
[62] Shamsudin NF, Ahmed QU, Mahmood S, Shah SAA, Sarian MN, Khattak MMAK, et al. Flavonoids as antidiabetic and anti-inflammatory agents: a review on structural activity relationship-based studies and meta-analysis. Int J Mol Sci 2022;23:12605.
[63] Mutoh M, Takahashi M, Fukuda K, Komatsu H, Enya T, Matsushima-Hibiya Y, et al. Suppression by flavonoids of cyclooxygenase-2 promoter-dependent transcriptional activity in colon cancer cells: structure-activity relationship. Jpn J Cancer Res 2000;91:686–91.
[64] Gao H, Nishioka T, Kawabata J, Kasai T. Structure-activity relationships for α-glucosidase inhibition of baicalein, 5, 6, 7-trihydroxyflavone: the effect of A-ring substitution. Biosci Biotechnol Biochem 2004;68:369–75.